Int J Adv Manuf Technol (2015) 77:1727–1740
DOI 10.1007/s00170-014-6507-y

ORIGINAL ARTICLE

An experimental investigation on surface finish in die-sinking EDM of Ti-5Al-2.5Sn

Md. Ashikur Rahman Khan · M. M. Rahman · K. Kadirgama

Received: 15 December 2013 / Accepted: 14 October 2014 / Published online: 16 November 2014

Abstract Electrical discharge machining (EDM) is a non-conventional process for shaping hard metals and forming deep and complex-shaped holes by spark erosion in all kinds of electroconductive materials. The choice of the electrical parameters on the EDM process depends impressively on workpiece-electrode material combination. In this research, an effort has been made to study the surface finish characteristics of the machined surface in EDM on Ti-5Al-2.5Sn titanium alloy. The microstructure of the machined surface is investigated for discharge energy and electrode materials. The peak current, pulse-on time, pulse-off time, servo-voltage and electrode material (copper, copper–tungsten and graphite) are considered as process variables. The experimental work was performed based on an experiment design (central composite design). The surface roughness (SR) increases with peak current and pulse-on time and decreases with servo-voltage. Besides, the effect of the process parameters on surface roughness depends on electrode material. At low discharge energy, copper–tungsten electrode produces the finest surface structure whilst graphite delivers worst surface characteristics. Copper–tungsten with low discharge energy (low peak current and pulse-on time) can be used to obtain better surface finish.

Keywords EDM · Surface finish · Ti-5Al-2.5Sn · Electrode materials · Process variables

M. A. R. Khan (✉)
Department of Information and Communication Technology, Noakhali Science and Technology University, Noakhali 3814, Bangladesh
e-mail: ashik.nstu@yahoo.com

M. M. Rahman · K. Kadirgama
Faculty of Mechanical Engineering, Universiti Malaysia Pahang, 26600 Pekan, Pahang, Malaysia

1 Introduction

For more than 50 years, electrical discharge machining has been an important non-traditional machining process and a well-known machining technique [1]. In EDM, there is no direct contact between the tool and the workpiece and no substantial mechanical force, which eliminates mechanical stresses, chatter and vibration problems during machining [2]. EDM produces complex shapes and permits high-precision machining of any hard, difficult-to-cut, brittle or thin materials. On the other hand, Ti-5Al-2.5Sn is a grade-6 titanium alloy that is used in airframes and jet engines due to its good weldability, stability and strength at elevated temperatures. Besides, Ti-5Al-2.5Sn is also used for manufacturing steam turbine blades, autoclaves and other process equipment vessels operating up to 480 °C, high-pressure cryogenic vessels, aircraft engines, compressor blades, missile fuel tanks and structural parts operating for short times up to 600 °C, airframe and jet-engine parts, welded stator assemblies, and hollow compressor blades. Despite of its numerous applications, it is very difficult to machine Ti-5Al-2.5Sn titanium alloy with conventional machining techniques. Despite the huge number of applications of titanium alloys, there is a key problem regarding machining using conventional machining processes [3]. However, the non-conventional process as electrical discharge machining can machine this titanium alloy effectively [4]. On the other hand, there are a number of process parameters that affect the EDM performance characteristics. Again, the investigation with regard to surface finish characteristics in EDM on Ti-5Al-2.5Sn titanium alloy is not explored yet, although the EDM performance characteristics have been studied for numerous materials.

Pradhan and Biswas [5] studied the surface roughness of AISI D2 tool steel for copper electrode. They investigated that surface roughness increases as peak current and pulse-on time increase. Surface roughness decreases with an increase in

pulse-off time. Insignificant variation in surface roughness was found with change in voltage. Tomadi et al. [6] studied the effectiveness of EDM process on tungsten carbide with copper–tungsten electrode. They found that the most influential factor is voltage, followed by the pulse-off time, whilst the peak current and pulse-on time do not significantly affect surface roughness. This observation contradicts the result obtained by Pradhan and Biswas [5] in regards of voltage. It was revealed that the surface roughness and average white layer thickness increase with the increasing of current and pulse duration in EDM of Ti-6Al-4V titanium alloy [7]. Experimental study was performed to investigate the effects of discharge current, pulse-on time, duty cycle and gap voltage on the EDM performance of the AlSiTi ceramic composite [8]. It was observed that the pulse-on time influences the surface roughness to a larger extent than other factors such as discharge current, duty cycle, and gap voltage.

Experiments were carried out on the performance of electrical discharge machining on AISI P20 tool steel [9]. The experiments were performed with graphite and copper as tool electrodes. It was noticed that the performance of any electrical discharge machining operation greatly depends on the thermophysical properties of the electrode material. Peak current, pulse duration and electrode (tool) polarity were found as more significant EDM variables. The best surface roughness was obtained for copper electrode. Beri et al. [10] carried out an experimental study of EDM of AISI D2 steel and found that surface roughness is less with a copper–tungsten electrode as compared with a conventional copper electrode. In EDM of tungsten carbide, it was found that silver–tungsten electrodes produced a smoother surface with the lowest roughness amongst tungsten, copper–tungsten and silver–tungsten electrodes [11]. An experimental investigation was carried out using four electrodes—copper, copper–tungsten, brass, and aluminium—to study EDM characteristics of En-31 tool steel [1]. Of the four tested electrode materials, it is observed that copper–tungsten offers comparatively low values of surface roughness at high discharge currents. Copper and aluminium electrodes produce high surface roughness at high values of current. Tsai et al. [2] perceived that that copper metal electrode machining yields lower surface roughness as well as more micro-cracks on the surface compared with a copper–chromium composite electrode. An experimental study was conducted to investigate the effect of the machining parameters on machining characteristics in EDM of tungsten carbide [12]. Experiments on tungsten carbide material were carried out with copper, copper–tungsten and graphite electrodes. However, they varied only peak current as parameter settings for all three electrodes. It was observed that the machined workpiece surface roughness increases with increasing peak current for all the three electrode materials. In EDM of tungsten carbide, copper exhibits the best performance as regards surface finish, followed by copper–tungsten, whilst graphite gives the poorest surface. Distinct electrodes of graphite, copper and aluminium were used in EDM of titanium alloy Ti-6Al-4V [7]. The aluminium electrode exhibits the best performance in terms of surface finish, whilst graphite shows the poorest performance in this regard. The copper electrode produces SR values between those obtained by aluminium and graphite electrodes. A relationship was also observed between wear on the electrode and the surface roughness of the workpiece for the machining of 40CrMnNiMo864 tool steel (AISI P20) [13].

It was stated that spark-affected layers are produced on steel by electrical discharge machining [14]. A multilayered heat-affected zone is created at the surface of workpiece when machining a workpiece with EDM. The recast layer, the outer region of the heat affected zone, consists of superimposed strata derived from melted and resolidified workpiece material. The recast layer that is formed on steels consists mostly of iron carbides in acicular or globular form, distributed within an austenite matrix, which are independent of the composition of the base material and of the type of the electrode.

The most recent research works about performance characteristics of electrical discharge machining that are carried out by distinct researchers are shown in the subsequent clause. Jung and Kwon [15] attempted to find the optimal machining conditions under which the micro-hole can be formed to a minimum diameter and a maximum aspect ratio. They conducted electrical discharge machining on SS304 material applying WC electrode. Experiment was accomplished allowing for voltage, capacitance, resistance, feed rate and RPM as process variables. Voltage and capacitance were found to be the most significant controlling parameters. Experiment was carried out on the influence of four factors—current, open-circuit voltage, servo and duty cycle over surface roughness on the electrical discharge machining of AISI 304 stainless steel [16]. In the case of surface finish, current was found the most influential factor amongst these four factors. Joshi and Pande [17] proposed a model to establish a relation between input variables (current, discharge voltage, duty cycle and discharge duration) and the process responses including shape of the crater. They conducted experiments on the die-sinking EDM machine considering AISI P20 mold steel and copper as work material and tool material, respectively. The obtained result evidenced that surface roughness initially increases with discharge current and then tapers off. Investigation was carried out on alloying capability of composite electrode, Cu-TaC, during electrical discharge machining on alpha–beta titanium alloy (Ti-6Al-4V) [18]. It was revealed that the machined surface was alloyed with carbides and oxides. The surface topography and the surface roughness are both affected by the machining conditions—peak current and pulse duration. A model was developed to determine the surface roughness for the parameters of current intensity, electrode type (copper and graphite) and workpiece material [19]. In this

research, two types of workpiece material, 50CrV4 and X200Cr15, were considered. It was explored that current intensity is the main influencing factor on surface roughness. The surface roughness contours are useful in determining the optimum cutting conditions. Copper tools produced a better surface quality than that obtained by a graphite tool. Gostimirovic et al. [20] experimentally investigated the thermal properties of the discharge energy on the EDM performance characteristics varying discharge current and pulse duration. The experiment was conducted using copper as electrode and manganese–vanadium tool steel, ASTM A681, as work material. In this study, the non-traditional dielectric fluid, petroleum, was used. They illustrated that the discharge power is more significant than discharge duration. Surface roughness directly depends on the discharge energy so that the discharge power and discharge duration cause a uniform increase of surface roughness. In another paper, Gostimirovic et al. [21] analysed the characteristics of electrical pulse parameters, namely discharge current and pulse duration. Experiment was conducted on manganese–vanadium tool steel utilizing graphite as electrode material. They revealed that the surface roughness directly depended on the discharge current and pulse duration; however, the discharge current is more significant than pulse duration. It was attempted to study the effects of voltage, current, pulse-on time and pulse-off time on surface roughness of NiTi alloy using copper tool and deionized water as a dielectric [22]. The results reveal that the pulse-on time and pulse-off time have the highest impact on surface roughness. With the increase of pulse current in NiTi alloy, surface roughness increases. The increase of voltage results in large surface pits that deteriorate the surface quality. The machining performance characteristics were investigated for mild steel workpiece using copper as electrode [23]. In this work, experiment was performed taking into account only single parameter, discharge current. It was shown that as the current increases, the temperature between the electrode and workpiece increases resulting in more vaporization of workpiece material. Pawade and Banwait [24] reviewed the research works carried out in the development of die-sinking EDM within the past decades for the improvement of machining characteristics. They also proposed Programmable Logic Controller (PLC)-based flexible machine controller to enhance the machining characteristics and to achieve high-level automation.

It is apparent from the prior researches that the electrical discharge machining performance characteristics mainly surface finish (surface roughness and/or surface structure) has been studied for distinct materials such as AISI D2 tool steel, tungsten carbide, Ti-6Al-4V titanium alloy, AlSiTi ceramic composite, AISI P20 tool steel, AISI D2 steel, En-31 tool steel, 40CrMnNiMo864 tool steel (AISI P20) and so on. However, the investigation with regard to surface finish characteristics in EDM on Ti-5Al-2.5Sn titanium alloy is still lagging. On the other hand, the EDM performance characteristics are not identical for all workpiece-electrode material combination. In the preceding researches, various process variables and different types of electrode materials are not considered simultaneously for a particular material. In this context, an effort has been made to study the surface finish characteristics of the machined surface in EDM on Ti-5Al-2.5Sn titanium alloy. The surface finish comprises surface roughness (R_a) and microstructure of the machined surface. The microstructure of the surface are analysed for distinct discharge energies and several electrodes. In the present study, peak current, pulse-on time, pulse-off time and servo-voltage are considered as process variables. Experiments are performed varying all these process variables for three electrode materials such as copper, copper–tungsten and graphite.

2 Experimental procedure

2.1 Process parameters

One of the most important and frequently used output parameters of the process is the surface roughness [25, 26]. Accordingly, surface roughness was set as the output parameter of the EDM experiment. Besides, the microstructure of the machined surface was set as objective function in this study. Surface roughness is a measure of the texture of a surface. The surface texture is the sum of all irregularities caused by roughness, waviness, and flaws. Roughness is the set of finer irregularities on the surface of a solid material, including flaws and tool marks caused by the manufacturing techniques used to produce the surface [27]. The surface roughness of the workpiece can be expressed by arithmetic average (R_a). The surface is rough when the deviation is large, and the surface is smooth when the deviation is small. Roughness average (R_a) is quantified in micrometres (μm) [27]. It can be estimated using Eq. (1) [5].

R_a=average deviation of profile $y(x)$ from the mean line

$$R_a = \frac{\text{Total shaded area}}{\text{L}}$$
$$R_a = \frac{1}{L}\int_0^L |y(x)|dx \quad (1)$$

where L is the sampling length, y is the profile curve and x is the profile direction.

In EDM, there are large numbers of machining parameters which can be varied in the EDM process which have different effects on the EDM performance characteristics [26]. EDM machining parameters are divided into two groups: non-electrical parameters (injection flushing pressure and rotational speed of electrode, electrode and workpiece material) and electrical

parameters (peak current, polarity, pulse duration and power supply voltage) [6]. It has been reported that the most important variables are the peak current, duration of the current pulse, open voltage of the gap, polarity of the electrode, thermodynamic properties of the tool and workpiece and physical properties of the tool and workpiece [28]. The workpiece and electrode material are the most influential factors amongst the non-electrical parameters. Eventually, the peak current, pulse-on time, pulse-off time, servo-voltage and tool materials were selected as the process variables for the present research. Copper, copper–tungsten and graphite were chosen as tool (electrode) materials.

The peak current is the maximum current available for each pulse during spark. It is applied between the electrode and the part to be machined and is measured in units of ampere. The mean of the amperage in the spark, measured for a complete cycle, is the average current. The peak current is the most commonly considered parameter in the EDM process and is symbolized by I_p [29]. In the electrical discharge process, every pulse comprises on time and off time, and these are expressed in microseconds (μ_s). Once the insulation condition between the electrode and the workpiece is broken down, current starts to flow; the pulse-on time (T_{on}) is the period from the commencement of the current flow to the end of discharge. Pulse-off time (T_{off}) is the duration of time (μs) between two successive pulse durations. Pulse-off time can be defined as the period between the ending of discharge and the beginning of the next discharge [30]. The EDM machine remains at temporary rest during the pulse-off time. It must be reasonably long so that the plasma caused by previous pulse discharge can be deionized [31]. In the EDM process, the servo motion is controlled in accordance with gap-voltage fluctuation relative to servo-voltage. Once the gap voltage is higher than the servo-voltage, the electrode advances for machining. In contrast, when the servo-voltage is higher than the gap voltage, the electrode retracts to open the gap. The servo-voltage is denoted as S_v and is measured in volts.

2.2 Workpiece preparation and experimentation

Ti-5Al-2.5Sn titanium alloy has been selected as workpiece materials in this research. The titanium alloy Ti-5Al-2.5Sn (grade-6) is available commercially in many forms. As a fundamental requirement, the electrode material should possess high thermal conductivity, superior melting and evaporation point and the ability to be easily machined [11]. Therefore, copper, copper–tungsten and graphite are chosen as electrode materials for the present study. The physical properties of these electrode tools are presented in Table 1 [7, 11, 12, 32].

Table 1 Physical properties of copper, copper–tungsten and graphite electrodes

Properties	Material		
	Copper	Graphite	Copper–tungsten
Density (g/cm^3)	8.904	1.77	15.2
Melting point (°C)	1083	3350	3500
Thermal conductivity (W/mK)	388	160–230	160
Porosity (%)	–	14–22	–

The workpiece material is titanium alloy Ti-5Al-2.5Sn with a size of 22 mm × 22 mm × 20 mm. The surface of each specimen was ground with 300–800 mesh emery paper to ensure parallelism, cleanliness and surface quality before conducting the experiment. The cylindrical copper, copper–tungsten and graphite electrodes of 100 mm × Ø20 mm were cut at a size of 25 × Ø20 mm by a section cut-off machine of Model MSX200M. Then, to achieve a mirror surface, the electrode specimens were machined on an engine lathe. The end faces of the electrode were ground using emery paper in the succession of 600, 800, and 1200 mesh to assure flatness and surface finish.

A number of experiments were carried out consistent with the design matrix obtained from central composite design. The peak current, pulse-on time, pulse-off time and servo-voltage were varied from 1–29 A, 10–350 μs, 60–300 μs and 75–115 V, respectively, during experiments. The design matrix using coded and uncoded values of the selected EDM parameters are presented in Table 2. EDM was carried out in accordance with this design matrix.

The value of arithmetic average surface roughness (R_a) was assessed using the Perthometer S2 from Mahr, Germany. Five observations were carried out on different positions of the machined surface for each sample, and the average of these five was taken as the value of surface roughness, R_a. Surface texture analysis was carried out by scanning electronic microscopy to observe the surface topography of selected specimens. For this purpose, the specimens were prepared after experiments as shown in Table 3. During the experiment, pulse-off time and servo-voltage were kept constant. Subsequently, the microstructure of the workpiece surface was investigated using SEM model-EVO 50 from Zeiss, Germany. All specimens were analysed with regard to all three electrode materials, namely copper, copper–tungsten and graphite. SEM micrographs are attained from the machined surface at different magnification sizes such as ×500 and ×1000. The surface characteristics are investigated for distinct discharge energies as well as the SEM micrographs are analysed considering all electrodes collectively to explore the effect of the electrode.

Table 2 Set of designed experiments for different parameters

Run order	Coded units				Uncoded units			
	I_p (A)	T_{on} (μs)	T_{off} (μs)	S_v (V)	I_p (A)	T_{on} (μs)	T_{off} (μs)	S_v (V)
1	0	0	0	0	15	180	180	95
2	−1	1	1	−1	8	265	240	85
3	2	0	0	0	29	180	180	95
4	0	0	0	0	15	180	180	95
5	0	0	0	−2	15	180	180	75
6	0	0	0	0	15	180	180	95
7	−1	−1	−1	−1	8	95	120	85
8	1	1	1	−1	22	265	240	85
9	−1	1	1	1	8	265	240	105
10	0	0	0	0	15	180	180	95
11	−1	−1	1	1	8	95	240	105
12	0	0	−2	0	15	180	60	95
13	−1	1	−1	−1	8	265	120	85
14	1	−1	−1	1	22	95	120	105
15	1	−1	1	1	22	95	240	105
16	−1	−1	−1	1	8	95	120	105
17	1	1	1	1	22	265	240	105
18	1	1	−1	−1	22	265	120	85
19	−2	0	0	0	1	180	180	95
20	0	0	0	0	15	180	180	95
21	0	0	2	0	15	180	300	95
22	0	0	0	0	15	180	180	95
23	1	−1	1	−1	22	95	240	85
24	1	1	−1	1	22	265	120	105
25	1	−1	−1	−1	22	95	120	85
26	0	0	0	2	15	180	180	115
27	−1	1	−1	1	8	265	120	105
28	0	−2	0	0	15	10	180	95
29	−1	−1	1	−1	8	95	240	85
30	0	2	0	0	15	350	180	95
31	0	0	0	0	15	180	180	95

3 Results and discussion

3.1 Surface roughness

The effect of each of the process parameters—peak current, pulse-on time, pulse-off time and servo-voltage—on the surface roughness in EDM of titanium alloy Ti-5Al-2.5Sn is discussed in this section. This is studied by varying one input parameter between its minimum and maximum value whilst the other input parameters are retained fixed in their reference condition. The reference condition is the mean value of the parameter. The effort has also been made to illustrate the effects of copper, copper–tungsten and graphite electrodes on surface roughness. Figures 1, 2, 3 and 4 describe the effect of the type of electrode material on surface roughness for varying peak current, pulse-on time, pulse-off time and servo-voltage. It is apparent from Fig. 1 that the surface roughness increases gradually with increasing peak current. As the pulse current is increased, deeper craters are more evident and rougher surfaces are more pronounced. The increase of discharge current increases the discharge energy, which promotes melting and vaporization of the workpiece material and generates larger and deeper craters, thus producing a higher surface roughness. Low discharge current creates small craters, resulting in lower material removal rate and hence leading to a smooth surface finish [5]. Thus, the surface finish of the workpiece deteriorates with an increase of peak current, and a smooth surface finish is achieved at low ampere. A similar observation was reported in previous studies [14]. Some researchers also depicted that the surface roughness is increased by increasing discharge current [7, 13, 14]. However, Rao et al. [16] and Joshi and Pande [17] illustrated that the surface roughness initially increases with discharge current and then tapers off. Similar trend of variation of crater depth with discharge current was observed in the research of Joshi and Pande [33]. However, they did not show the reasons of such effect. This distinction can be explained through two reasons—one is the change of workpiece and tool material since the EDM characteristics are greatly associated with workpiece and tool material and the other one is the effect of interaction of discharge current and voltage.

Figure 1 shows that the surface roughness increases linearly as the peak current increases for copper and copper–tungsten electrodes. However, for positive graphite electrode, the surface roughness increases gradually up to 15 A and beyond this range; a disparate characteristic of surface roughness is appeared with the increase of peak current. The results indicate that the most even surface finish is achieved with a copper electrode at low peak current (<9 A), whilst copper–tungsten exhibits the best performance at high peak current (>9 A). On the other hand, although the graphite electrode gives the

Table 3 Set of designed experiments for SEM viewing

Sl no.	Peak current (A)	Pulse-on time (μs)	Pulse-off time (μs)	Servo-voltage (V)
1	15	180	120	85
2	29	320	120	85
3	2	95	120	85

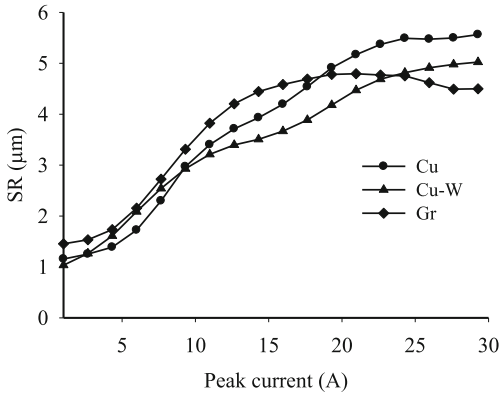

Fig. 1 EDM outputs for varied input peak current

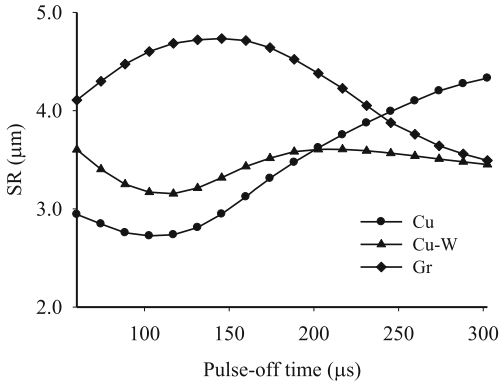

Fig. 3 EDM outputs for varied pulse-off time

poorest surface amongst the three electrode materials, it provides the minimum surface roughness when the peak current is above 23 A. The high ampere causes high temperature, which generates more discharge energy. This high temperature melts the copper electrode more since its melting point (1083 °C) is much lower than that of copper–tungsten (3500 °C) and graphite (3350 °C). Some of the electrode material particles fall on the workpiece surface resulting in a rougher surface. As a consequence, the copper–tungsten electrode produces a smooth and fine surface compared with the copper and graphite electrodes at high ampere. Lee and Li [12] reported that copper–tungsten electrodes provide better surface finish compared to graphite electrodes in EDM on tungsten carbide. Lee and Li [12] also found that the copper tool gives the best surface attributes, whilst graphite gives the poorest surface. Conversely, Singh et al. [1] mentioned that copper–tungsten yields low values of surface roughness at high discharge current compared with copper electrode in EDM on EN-31 tool steel. Machining with graphite electrode is more stable as a cathode than anode, and it will be discussed in the subsequent section [9]. Unlike copper and copper–tungsten electrode, a decreasing trend of tool wear of graphite electrode is observed with the increase in the peak current when the peak current is above 25 A. The surface roughness also depends on tool wear, and the lower tool causes lower surface roughness. Thus, the positive graphite provides the minimum surface roughness at high peak current (>23 A).

The effect of pulse-on time on surface roughness characteristics is shown in Fig. 2. It is seen that initially, the surface roughness increases until a specific (peak) value and then retains constant when the pulse-on time increases for graphite electrode. On the other hand, after the peak value of SR, the surface roughness decreases as the pulse-on time increases for copper and copper–tungsten electrodes. The discharge energy is directly related to the pulse-on time in such way as the pulse-on time increases, the discharge energy increases [5]. The high discharge energy creates more craters and enhances material removal. Therefore, the surface roughness increases as the pulse-on time increases. However, the too long pulse-on time causes arcing and reduces the material removal [12]. The energy density within the discharge spot is reduced on account of the expansion of discharge column at a longer pulse-on time. As a result, small craters are produced at too long pulse-on time. Thus, the decreasing tendency is apparent to too long pulse-on time. The fine surface finish of the EDM machined surface is achieved at low pulse-on time. The same results are reported by Hascalik and Caydas [7]; Kiyak and Cakir [13]. Though Patel et al. [8] illustrated that surface roughness initially increases and then decreases with increasing pulse-on time, Ndaliman et al. [18] investigated that the lower the

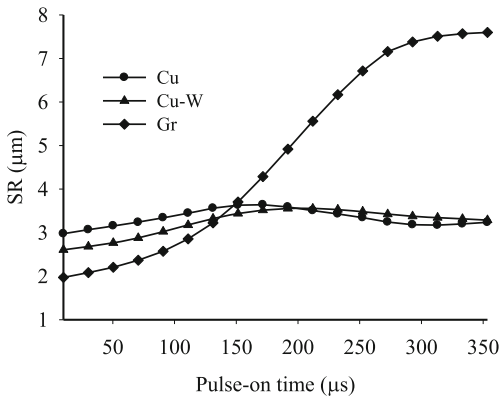

Fig. 2 EDM outputs for varied pulse-on time

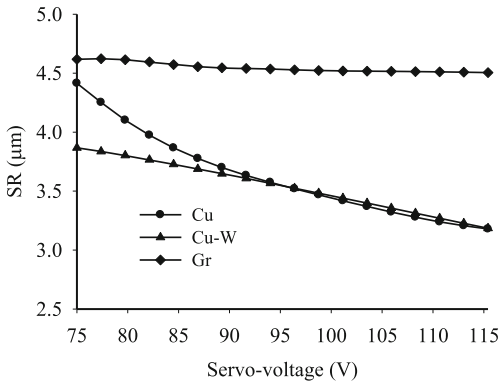

Fig. 4 EDM outputs for varied servo-voltage

pulse-on time, the lower the surface roughness. On the contrary, a dissimilar effect was investigated by Daneshmand et al. [22] as the surface roughness primarily decreases and then increases with pulse-on time.

Figure 3 shows the impact of pulse-off time on surface roughness. The diverse impact of the pulse-off time on surface roughness characteristics is apparent in this study. As can be seen from the figure, an increase in pulse-off time initially reduces surface roughness and thereafter causes increased surface roughness. Then again, an increasing and a falling tendency of the surface roughness graph are observed as pulse-off time is increased for copper and copper–tungsten electrode, respectively. It is interesting to note that the trends of surface roughness for graphite are opposite to those of copper and copper–tungsten electrode. When the pulse-off time is too short, there is not enough time to clear the disintegrated particles from the gap between the electrode and the workpiece [12]. If the pulse-off time is too short, an unstable spark discharge can be easily induced because of insufficient insulation recovery [30]. On the other hand, a long pulse-off time influences the cooling effect on the electrode and workpiece surface, and more energy is required to establish the plasma channel; consequently, there is a higher surface roughness. Accordingly, it is obvious that the pulse-off time must be sufficiently long to acquire a uniform erosion of material from the surface of the workpiece and stable machining process; otherwise, a non-uniform erosion of the workpiece surface will occur. Thus, disparate effects of pulse-off time on surface finish have been observed. In addition, it is understood that EDM necessitates a suitable pulse-off time to achieve a fine surface finish. Tomadi et al. [6] observed rougher surfaces at higher pulse-off time; conversely, Pradhan and Biswas [5] reported that surface roughness decreases as pulse-off time increases. On the other hand, Daneshmand et al. [22] investigated that surface roughness primarily increases and then decreases with increasing pulse-off time.

The thermophysical properties of the electrode material control the performance of the electrical discharge machining operation, although the non-thermal properties (mechanical and electrodynamic effects) are unavoidable. In terms of thermophysical properties, graphite is very different from other electrodes such as copper and copper–tungsten [9]. The discharge current occurs following the breakdown of the open-circuit voltage. This phenomenon is only possible when the cathode electrode begins to emit electrons. The copper acting as a cathode is able to emit electrons when some of it is melted and vaporized. However, graphite as a cathode can emit electrons below its sublimation temperature. Consequently, graphite is more stable as a cathode, whilst copper is more stable as an anode. Thus, the trends of surface roughness for a graphite electrode are opposite to those of the other two electrodes.

It is apparent from Fig. 4 that as the servo-voltage increases, surface roughness decreases. When the gap voltage is higher than the servo-voltage, the electrode advances for machining and, in contrast, once the servo-voltage is higher than the gap voltage, the electrode retracts to open the gap [31]. Through a servo reference system, the servo-voltage controls the spark gap, which is the distance between the electrode and the workpiece during the process of EDM [6]. The machining gap between the electrode and the workpiece increases as the servo-voltage increases. At high servo-voltage, the electrode is no longer able to advance towards the workpiece, resulting in a decrease in discharge. Besides, a high servo-voltage allows a lower time for the cutting operation. Thus, an increase in servo-voltage reduces the amount of crater formation. On the other hand, higher servo-voltage reduces the size of craters. Moreover, it facilitates the washing of debris away from the gap and reduces the tendency of arcing and short-circuit occurrences. Therefore, the surface roughness decreases with an increase of servo-voltage, and a higher value of servo-voltage presents a more even surface on the workpiece.

3.2 Surface topography

The surface topography of a number of samples is investigated using scanning electronic microscopy for qualitative analysis (surface characteristics) of the machined surface. These samples were machined with varying discharge energy (pulse current×pulse-on time such as 2 A×95 μs, 15 A×180 μs, and 29 A×320 μs) and electrodes (copper, copper–tungsten and graphite). Pulse-off time (120 μs) and servo-voltage (95 V) were kept constant during the machining. SEM micrographs are acquired from the machined surface at magnifications of ×500 and ×1000. The surface characteristics are investigated for distinct discharge energies. Then the SEM micrographs are analysed considering all electrodes collectively to explore the effect of the electrode.

Scanning electronic microscopic views of the surface topography of the specimen machined with a copper electrode are shown in Fig. 5 for distinct discharge energy. A layer containing numerous pock marks, globules, craters, microcracks and cracks is visible on the machined surface. SEM reveals small, shallow craters, a few micro-cracks and globules of debris on the surface, as shown in Fig. 5a. Besides, the machined surface is characterized by scattered and small debris. The spark occurring through the high-temperature plasma melts and vaporizes a small area of the workpiece surface, and ultimately, craters are formed. The crater size depends on the pulse current as well as the discharge energy. When the pulse-on time is small, the frequency (discharges per second) is high. Low peak current and high frequency correspond to low material removal, which results in smaller craters [1, 13]. SEM reveals the presence of micro-cracks resulting from solidification and/or rapid cooling of the recast layer. The intense heat generated by each discharge produces

severe temperature gradients in the machined surface. At the end of discharge, the surface layer is rapidly cooled by the dielectric fluid and develops a residual tensile stress. Cracks are formed when the residual tensile stress in the surface exceeds the ultimate tensile strength of the material [34]. The unexpelled melted material resolidifies after rapid cooling by the dielectric fluid and forms globules of debris. Some of these are very small and attached to the surface, appearing like pockmarks. Thus, low discharge energy creates small and shallow craters, micro-cracks and globules.

According to the SEM image in Fig. 5, the size and depth of the discharge craters increase as the discharge energy level increases. It is revealed that the number of globules decreases as the energy intensity increases. The increase of discharge current and pulse-on time increases the discharge energy. The rate of melting and vaporization is increased, resulting in a greater material removal [35]. The long pulse-on time is responsible for larger craters; however, a strong peak current causes deep craters at high discharge energy. Therefore, high discharge energy produces deeper and wider craters, generating a rougher surface. The globule formation depends on the erosion of the electrode, which in turn depends on the discharge energy. The high discharge energy produces an inhibitor carbon layer on the electrode surface. This carbon layer reduces the electrode wear [26]. The high discharge energy causes a large impulsive force, which can remove more debris from the machining gap [8]. Thus, the surface topography with high discharge energy presents a smaller number of globules and pock marks.

The increase in pulse-on time increases the white layer thickness and residual stress. A larger amount of heat energy penetrates into the interior of the material at long pulse-on time. The temperature of the machined surface reaches the melting point readily. The molten material resolidifies following rapid cooling (quenching) by the dielectric fluid and

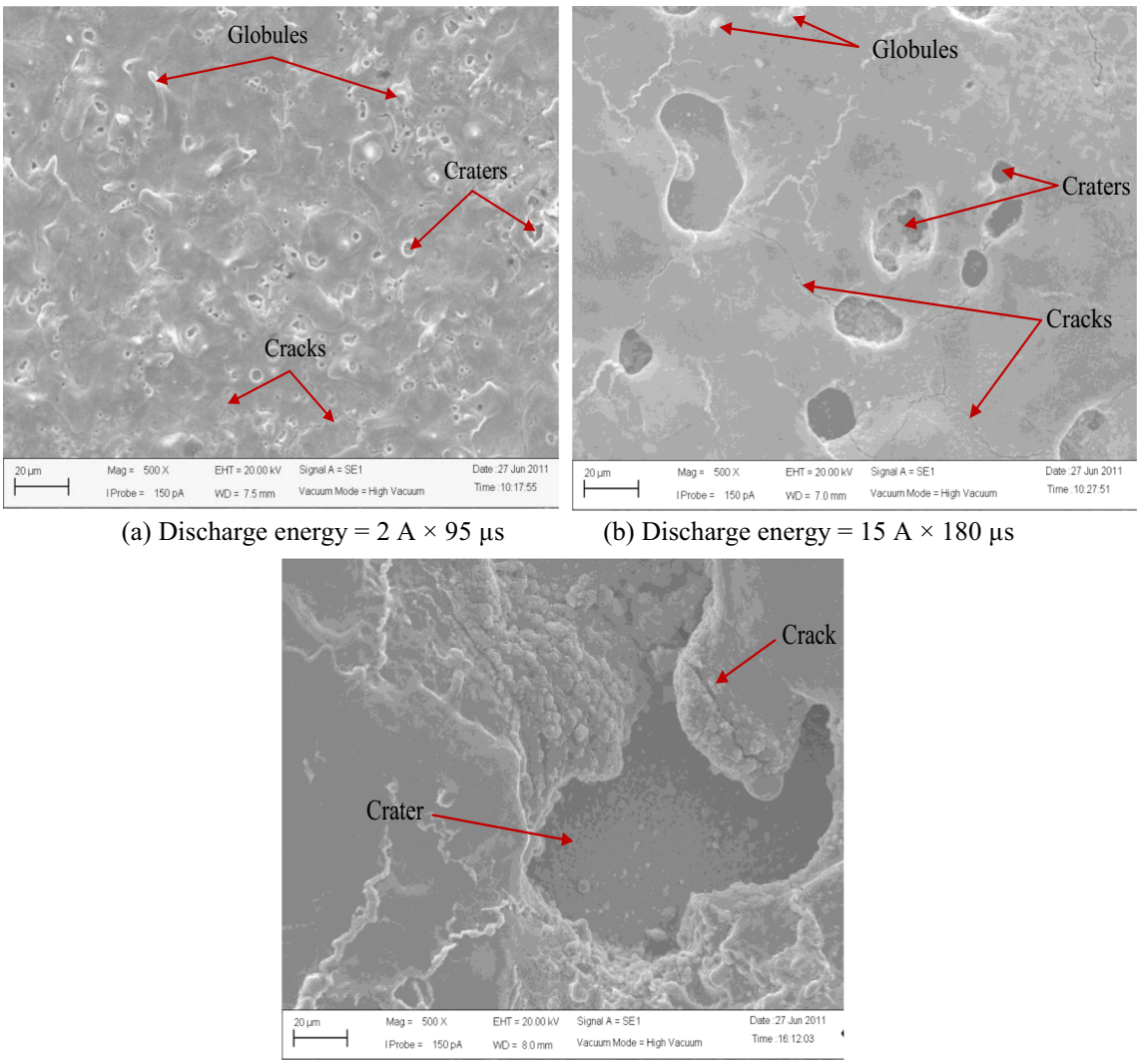

(a) Discharge energy = 2 A × 95 µs (b) Discharge energy = 15 A × 180 µs

(c) Discharge energy = 29 A × 320 µs

Fig. 5 SEM micrographs of the machined surface with Cu electrode

produces a thick recast layer [36]. At the same time, the severity of the crack opening increases, reducing the effective length of the surface cracks. Thus, the high discharge energy produces a greater degree of cracks with wide openings.

The surface topography of the machined surface with a Cu-W electrode is presented in Fig. 6 for distinct discharge energy. The surface is characterized by craters, globules of debris, cracks and pockmarks together with a recast layer. The discharge energy supplied to the machining zone melts and vaporizes the material from the workpiece surface, creating numerous minute craters. The molten material is not removed completely owing to inadequate flushing through the micro-gap between the electrode and workpiece and insufficient impulsive force [36]. Thus, the remaining molten material is cooled rapidly and resolidifies on the surface to form globules. Cracks are formed due to the solidification of the recast layer and increased residual stresses in the machined surface caused by rapid cooling. Cracks are formed when the residual stresses exceed the ultimate tensile strength of the base material [34].

The size of the craters and the degree of cracking increase as discharge energy increases. A high discharge energy increases the rate of melting and vaporization, which causes larger and deeper craters [35]. On the other hand, the high discharge energy results in a thick recast layer as well as increased residual stress at the machined surface. Thus, larger and deeper craters and a greater degree of cracking are evident at higher discharge energy.

A large number of globules are observed for higher discharge energy (29 A×320 μs) compared with lower discharge energy (15 A×180 μs). The higher discharge energy melts and vaporizes more material than lower discharge energy. The ratios of pulse-off time and pulse-on time are 0.375 (120/320) and 0.667 (120/180) for pulse-on times of 320 and 180 μs, respectively. Accordingly, the higher discharge energy (29 A×320 μs) results in a shorter time to eject the molten

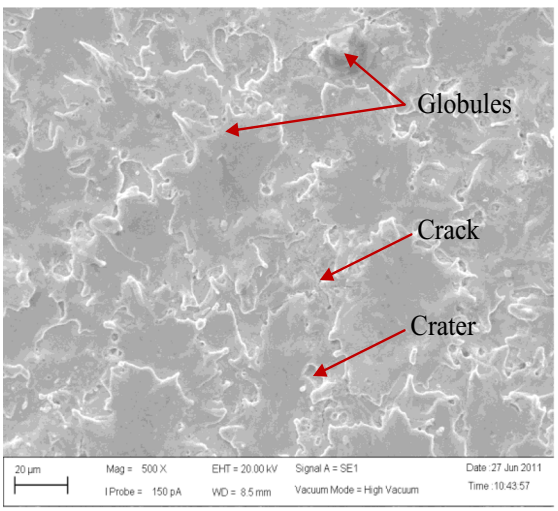

(a) Discharge energy = 2 A × 95 μs

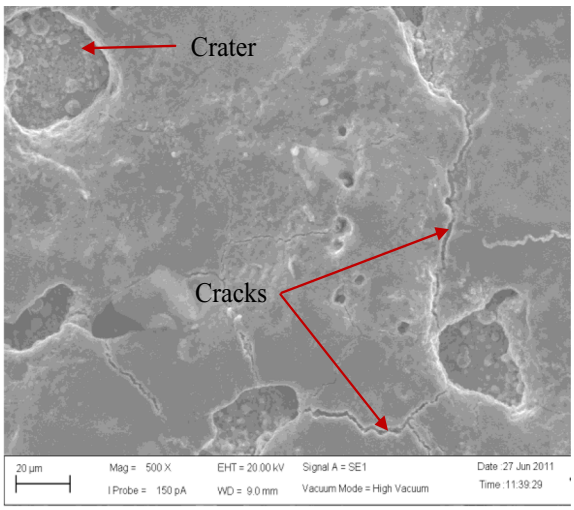

(b) Discharge energy = 15 A × 180 μs

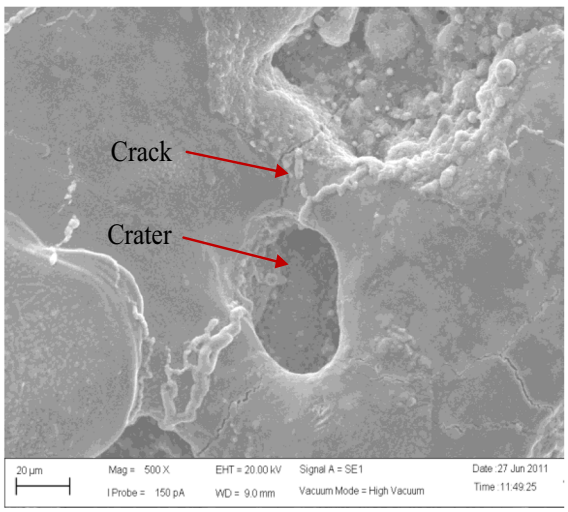

(c) Discharge energy = 29 A × 320 μs

Fig. 6 SEM micrographs of the machined surface with Cu-W electrode

material from the surface compared to lower discharge energy (15 A×180 μs). Hence, the molten material is not removed entirely from the surface. The remaining molten material is attached to the surface, creating a larger number of globules.

It is interesting to note that a lower discharge energy level (15 A×180 μs) carries a higher degree of cracking in combination with smaller craters as compared with higher discharge energy level (29 A×320 μs). When the discharge energy is high, the amount of material removed is increased, creating more craters. Similarly, at lower discharge energy, the amount of material removed is decreased, resulting smaller craters. On the other hand, the formation of enlarged craters and more globules cause a wide variation in the thickness of the white layer. Moreover, no significant increase in the induced stress is apparent at high peak current, signifying a lower degree of cracking [37]. Thus, a higher degree of cracking and small craters are apparent in Fig. 6b, and the opposite can be seen in Fig. 6c.

The surface topography of the machined surface generated during EDM with graphite electrodes is illustrated in Fig. 7 for distinct discharge energy. The machined surface is characterized by globules, craters, cracks and small debris like pockmarks. The reason for the formation of craters, globules and cracks has been clarified in the former sections. It is observed that the size of the crater and degree of crack increase as the discharge energy increases. It has also been discussed above.

The SEM micrographs of the machined surfaces are presented in Fig. 8 to compare the surface topography amongst different electrodes. Accordingly, it is appeared that the copper–tungsten electrode presents the lowest amount of craters and cracks when compared with the copper and graphite electrodes at the energy level of 2 A×95 μs and 15 A×180 μs. However, it is perceived that the copper–tungsten electrode shows a greater amount of globules, whereas the copper electrode reveals more craters at a lower energy level, 2 A×95 μs. On the other hand, the graphite electrode shows greater craters and a higher degree of cracks compared to the copper and copper–tungsten electrodes. However, copper electrode produces the largest size of crater followed by copper–tungsten, and graphite generates smallest size of craters along with high degree of crack at high discharge energy (29 A×320 μs). The surface texture of the workpiece surface during machining depends on tool electrode wear. High thermal conductivity of a material facilitates easy heat transfer through the body of the electrodes instead of being concentrated on the surface [38]. Accordingly, a small amount of heat is available for electrode wear at high thermal conductivity. On the other hand, a high melting temperature of a material results in low melting which means that there is low electrode wear. Although the copper–tungsten possesses lower thermal conductivity (160 W/mK) [11], it also facilitates low melting due to its higher melting temperature (3500 °C) [12]. Moreover, copper–tungsten resists wear because of its high density (15.2 g/cm^3) [12] where the particles are bonded with high compactness. In consequence, there is less wear of the electrode, and ultimately smaller craters and a lower number of cracks when EDM is used with the copper–tungsten electrode at 2 A×95 μs and 15 A×180 μs. The graphite electrode causes greater wear of the electrode material in spite of its lower thermal conductivity (160–230 W/mK) and high melting temperature (3350 °C) [12]. The graphite electrode is attributed with high porosity. The particles of graphite are not bonded with such high compactness since the density of graphite (1.77 g/cm^3) is remarkably low. As a result, the graphite electrode allows more wear. Thus, the SEM micrographs for graphite electrode reveal larger craters, a higher degree of cracking and more globules as compared to other electrodes when the discharge energies are 2 A×95 μs and 15 A×180 μs. The graphite electrode produces diverse characteristics on surface topography of the workpiece. Thus, graphite causes smaller craters along with a higher degree of crack than copper and copper–tungsten electrodes at the energy level of (29 A×320 μs). Then, the copper electrode permits rapid dissipation of heat through the sample, rather than being concentrated on the surface, because of its higher thermal conductivity (388 W/mK) [32, 38]. However, a great tendency to melt is evidenced in the case of the copper electrode owing to its low melting temperature, 1083 °C [12]. In addition, the density of the copper electrode material (8.9 g/cm^3) is between the densities of the copper–tungsten and graphite material [32]. Thus, the surface topography of the machined surface with the copper electrode depicts moderate surface characteristics between those of the copper–tungsten and graphite electrodes.

It is understood that the copper–tungsten electrode produces the finest surface structure whilst graphite delivers worst surface characteristics at the discharge energy of 2 A×95 μs and 15 A×180 μs. At high discharge energy (29 A×320 μs), graphite produces smallest size of craters but highest degree of crack whilst copper causes largest size of craters followed by copper–tungsten. It is also obvious that the copper–tungsten produces a better surface structure because of its high melting temperature as well as its high density. It is perceived from the analysis that the melting point, thermal conductivity and the density also significantly affect the electrode wear as well as the surface structure. Thus, an electrode material with high thermal conductivity, high melting point and high density can produce superior surface structures.

4 Conclusion

An extensive experimental study has been conducted to investigate the effect of the machining parameters on surface roughness and surface structure in EDM of Ti-5Al-2.5Sn titanium

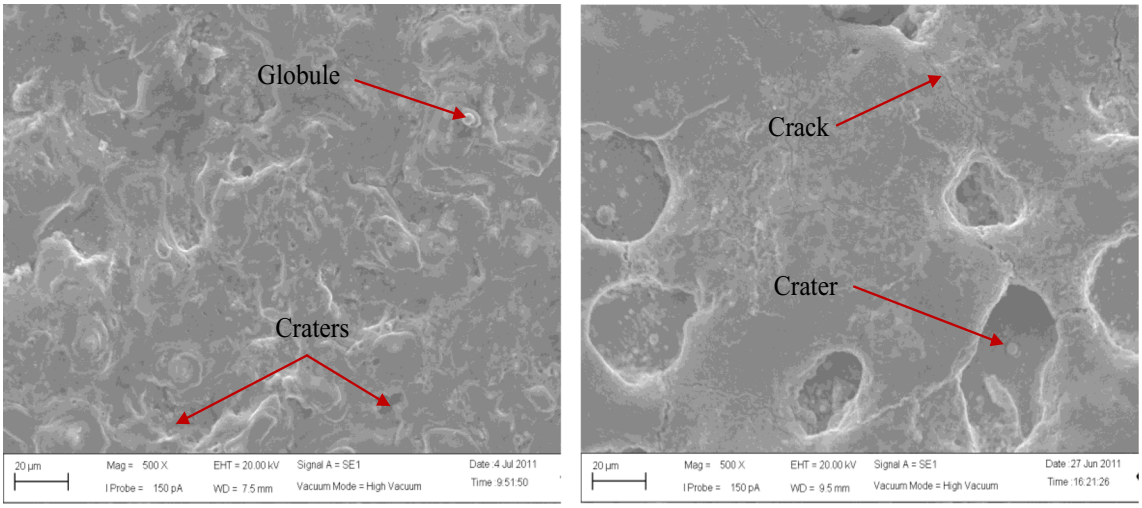

(a) Discharge energy = 2 A × 95 µs (b) Discharge energy = 15 A × 180 µs

(c) Discharge energy = 29 A × 320 µs

Fig. 7 SEM micrographs of the machined surface with Gr electrode

alloy. The machining parameters are the peak current, pulse-on time, pulse-off time, servo-voltage and electrode materials. The following conclusions can be drawn from the study.

It is apparent that the surface roughness increases linearly as the peak current increases for copper and copper–tungsten electrodes. However, for graphite electrode, the surface roughness increases gradually up to 15 A and beyond this range; a disparate characteristic of surface roughness is appeared with the increase of peak current. A smooth surface finish is achieved at low ampere for all electrodes. It is observed that copper electrode offers the most even surface finish at low peak current (<9 A), whilst the copper–tungsten exhibits the best performance at high peak current (>9 A). Although the graphite electrode produces the poorest surface amongst the three electrode materials, it provides the minimum surface roughness when the peak current is above 23 A.

It is seen that the surface roughness increases with the increase of pulse-on time until a certain value (peak). Initially, the surface roughness increases until a specific value and then retains constant as the pulse-on time increases for graphite electrode. For copper and copper–tungsten electrodes, after the peak value of SR, the surface roughness decreases as the pulse-on time increases.

In this study, the diverse effect of the pulse-off time on surface roughness characteristics is apparent. An increase in pulse-off time initially reduces surface roughness and thereafter causes increased surface roughness. Then again, an increasing and a falling trend of the surface roughness graph are found as pulse-off time is increased for copper and copper–tungsten electrode, respectively. However, the trends of surface roughness for graphite are opposite to those of copper and copper–tungsten electrode.

As the servo-voltage increases, the surface roughness decreases for all electrode materials, and a higher value of servo-voltage presents a more even surface on the workpiece.

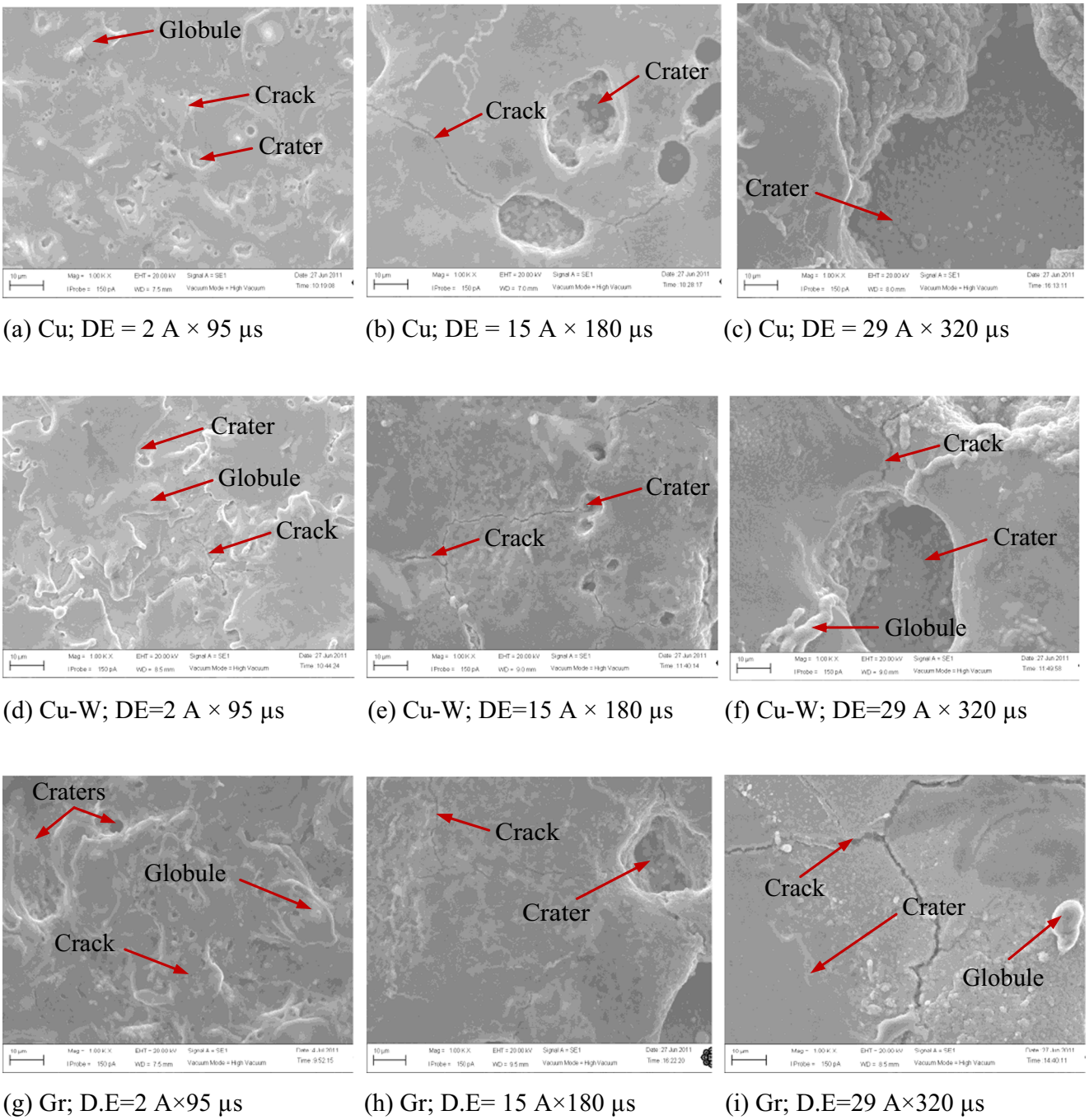

(a) Cu; DE = 2 A × 95 μs (b) Cu; DE = 15 A × 180 μs (c) Cu; DE = 29 A × 320 μs

(d) Cu-W; DE=2 A × 95 μs (e) Cu-W; DE=15 A × 180 μs (f) Cu-W; DE=29 A × 320 μs

(g) Gr; D.E=2 A×95 μs (h) Gr; D.E= 15 A×180 μs (i) Gr; D.E=29 A×320 μs

Fig. 8 SEM micrographs of the machined surface with different electrodes for altered discharge energy (D.E)

The SEM analysis evidences a layer on the machined surface which contains numerous pock marks, globules, craters, micro cracks and cracks. The size and amount of these characteristics vary with discharge energy. It is observed that as the discharge energy level increases, the size and depth of the discharge craters and degree of the crack increase whilst the amount of globules decreases. However, for copper–tungsten electrode, a lower discharge energy level (15 A×180 μs) carries a higher degree of cracking in combination with smaller craters as compared with the higher discharge energy level (29 A×320 μs).

Copper–tungsten electrode presents the lowest amount of craters and cracks when compared with the copper and graphite electrodes at the energy level of 2 A×95 μs and 15 A×180 μs. The graphite electrode shows greater craters, and a higher degree of cracks compared to the copper and copper–tungsten electrodes. On the other hand, copper electrode produces the largest size of the crater followed by copper–

tungsten, and graphite generates smallest size of craters along with the high degree of crack at high discharge energy (29 A× 320 μs).

It is understood that the copper–tungsten electrode produces the finest surface structure whilst graphite delivers worst surface characteristics at the discharge energy of 2 A× 95 μs and 15 A×180 μs. At high discharge energy (29 A× 320 μs) graphite produces the smallest size of craters but the highest degree of crack whilst copper causes largest size of craters followed by copper–tungsten.

Acknowledgments The authors would like to acknowledge the support of Universiti Malaysia Pahang.

References

1. Singh S, Maheshwari S, Pandey PC (2004) Some investigations into the electric discharge machining of hardened tool steel using different electrode materials. J Mater Process Technol 149:272–277
2. Tsai HC, Yan BH, Huang FY (2003) EDM performance of Cr/Cu-based composite electrodes. Int J Mach Tools Manuf 43:245–252
3. Rahman MM, Khan MAR, Kadirgama K, Noor MM, Bakar RA (2011) Optimization of machining parameters on tool wear rate of Ti-6Al-4V through EDM using copper tungsten electrode: A statistical approach. Adv Mater Res 152–153:1595–1602
4. Rahman MM, Khan MAR, Kadirgama K, Noor MM, Bakar RA (2010) Modeling of material removal on machining of Ti-6Al-4V through EDM using copper tungsten electrode and positive polarity. Int J Mech Mater Eng 1(3):135–140
5. Pradhan MK, Biswas CK (2009) Modeling and analysis of process parameters on surface roughness in EDM of AISI D2 tool steel by RSM approach. Int J Eng Appl Sci 5(5):346–351
6. Tomadi SH, Hassan MA, Hamedon Z, Daud R, Khalid AG (2009) Analysis of the influence of EDM parameters on surface quality, material removal rate and electrode wear of tungsten carbide. Proc Int MultiConf Eng Comput Sci 2:1803–1808
7. Hascalik A, Caydas U (2007) Electrical discharge machining of titanium alloy (Ti–6Al–4V). Appl Surf Sci 253:9007–9016
8. Patel KM, Pandey PM, Rao PV (2009) Determination of an optimum parametric combination using a surface roughness prediction model for EDM of Al2O3/SiCw/TiC ceramic composite. Mater Manuf Process 24:675–682
9. Amorim FL, Weingaertner WL (2007) The behavior of graphite and copper electrodes on the finish die-sinking electrical discharge machining (EDM) of AISI P20 tool steel. J Braz Soc Mech Sci Eng 29(4):367–371
10. Beri N, Maheshwari S, Sharma C, Kumar A (2008) Performance evaluation of powder metallurgy electrode in electrical discharge machining of AISI D2 steel using Taguchi method. Int J Mech Syst Sci Eng 2(3):167–171
11. Jahan MP, Wong YS, Rahman M (2009) A study on the fine-finish die-sinking micro-EDM of tungsten carbide using different electrode materials. J Mater Process Technol 209:3956–3967
12. Lee SH, Li XP (2001) Study of the effect of machining parameters on the machining characteristics in electrical discharge machining of tungsten carbide. J Mater Process Technol 115:344–358
13. Kiyak M, Cakir O (2007) Examination of machining parameters on surface roughness in EDM of tool steel. J Mater Process Technol 191:141–144
14. Amorim FL, Weingaertner WL (2004) Die-sinking electrical discharge machining of a high-strength copper-based alloy for injection molds. J Braz Soc Mech Sci Eng 26(2):137–144
15. Jung JH, Kwon WT (2010) Optimization of EDM process for multiple performance characteristics using Taguchi method and grey relational analysis. J Mech Sci Technol 24(5):1083–1090
16. Rao PS, Kumar JS, Reddy KVK, Reddy BS (2010) Parametric study of electrical discharge machining of AISI 304 stainless steel. Int J Eng Sci Technol 2(8):3535–3550
17. Joshi SN, Pande SS (2011) Intelligent process modeling and optimization of die-sinking electric discharge machining. Appl Soft Comput 11:2743–2755
18. Ndaliman MB, Khan AA, Ali MY (2011) Surface modification of titanium alloy through electrical discharge machining (EDM). Int J Mech Mater Eng 6(3):380–384
19. Salem SB, Tebni W, Bayraktar E (2011) Prediction of surface roughness by experimental design methodology in electrical discharge machining (EDM). J Achiev Mater Manuf Eng 49(2):150–157
20. Gostimirovic M, Kovac P, Sekulic M, Skoric B (2012) Influence of discharge energy on machining characteristics in EDM. J Mech Sci Technol 26(1):173–179
21. Gostimirovic M, Kovac P, Skoric B, Sekulic M (2012) Effect of electrical pulse parameters on the machining performance in EDM. Indian J Eng Mater Sci 18:411–415
22. Daneshmand S, Kahrizi EF, Abedi E, Abdolhosseini MM (2013) Influence of machining parameters on electro discharge machining of NiTi shape memory alloys. Int J Electrochem Sci 8:3095–3104
23. Raghav G, Kadam BS, Kumar M (2013) Optimization of material removal rate in electric discharge machining using mild steel. Int J Emerg Sci Eng 1(7):2319–6378
24. Pawade MM, Banwait SS (2013) A brief review of die sinking electrical discharging machining process towards automation. Am J Mech Eng 1(2):43–49
25. Khan MAR, Rahman MM, Kadirgama K, Maleque MA, Ishak M (2011) Prediction of surface roughness of Ti-6Al-4V in electrical discharge machining: A regression model. J Mech Eng Sci 1:16–24
26. Marafona J, Wykes C (2000) A new method of optimising material removal rate using EDM with copper–tungsten electrodes. Int J Mach Tools Manuf 40:153–164
27. Jones FD, Ryffel HH, Oberg E, McCauley CJ, Heald RM (2004) Machinery's handbook. Industrial Press, New York
28. Mohri N, Saito N, Tsunekawa Y (1993) Metal surface modification by electrical discharge machining with composite electrode. CIRP Ann Manuf Technol 42:219–222
29. Mahamat ATZ, Rani AMA, Husain P (2011) Machining of cemented tungsten carbide using EDM. J Appl Sci 11(10):1784–1790
30. Wu KL, Yan BH, Lee JW, Ding CG (2009) Study on the characteristics of electrical discharge machining using dielectric with surfactant. J Mater Process Technol 209:3783–3789
31. Kunieda M, Lauwers B, Rajurkar KP, Schumacher BM (2005) Advancing EDM through fundamental insight into the process. CIRP Ann Manuf Technol 54(2):64–87
32. Lin YC, Chen YF, Wang DA, Lee HS (2009) Optimization of machining parameters in magnetic force assisted EDM based on Taguchi method. J Mater Process Technol 209:3374–3383
33. Joshi SN, Pande SS (2009) Development of an intelligent process model for EDM. Int J Adv Manuf Technol 45(3):300–317
34. Senthilkumar V, Omprakash BU (2011) Effect of titanium carbide particle addition in the aluminium composite on EDM process parameters. J Manuf Process 13:60–66
35. Kathiresan M, Sornakumar T (2010) EDM studies on aluminum alloy-silicon carbide composites developed by vortex

technique and pressure die casting. J Miner Mater Charact Eng 9(1):79–88
36. Bonny K, De Baets P, Van Wittenberghe J, Delgado YP, Vleugels J, Van der Biest O, Lauwers B (2010) Influence of electrical discharge machining on sliding friction and wear of WC–Ni cemented carbide. Tribol Int 43:2333–2344
37. Lee HT, Tai TY (2003) Relationship between EDM parameters and surface crack formation. J Mater Process Technol 142:676–683
38. Rebelo JC, Dias AM, Mesquita R, Vassalo P, Santos M (2000) An experimental study on electro-discharge machining and polishing of high strength copper-beryllium alloys. J Mater Process Technol 103: 389–397